IEEE Access
Multidisciplinary | Rapid Review | Open Access Journal

Received March 17, 2020, accepted March 22, 2020, date of publication March 24, 2020, date of current version April 8, 2020.

Digital Object Identifier 10.1109/ACCESS.2020.2983106

Improved Fast Method of Initial Rotor Position Estimation for Interior Permanent Magnet Synchronous Motor by Symmetric Pulse Voltage Injection

ZIHUI WANG, ZEWEI CAO, AND ZHIYUAN HE
Zhejiang University of Science and Technology, Hangzhou 310023, China
Corresponding author: Zihui Wang (wzh2718@zust.edu.cn)

This work was supported in part by the Natural Science Foundation of Zhejiang Province, China, under Grant LQ17E070002.

ABSTRACT The precise information of initial rotor position is very important to high performance Interior Permanent Magnet Synchronous Machine (IPMSM) adopting incremental encoder, which can normally be obtained by the high-frequency (HF) rotating or pulsating voltage injection methods. However, the demodulation procedure may confront with the challenge of constrained stability and limited accuracy. For improving estimation accuracy, an improved impulse injection method with merits of simple and fast is proposed. It is carried out by generating a series of phase-axial injections to calculate the probable rotor position, then injecting two reciprocal voltage pulses to obtain the rotor polarity, and finally injecting iterative voltage vectors to obtain the real position rapidly. During the estimation process, the filters to extract the high frequency current signals are not needed. The method effectiveness is validated by the measured results of IPMSM test platform. In the same time, its application limitation is deduced by comparison with the measured results between IPMSM and surface-mounted PMSM (SPMSM). It is shown that the estimation algorithm is compatible with motor parameter differences and can reduce the influence of inductance saturation and nonlinear voltage error. Therefore, the proposed method not only improves the accuracy and robustness of the PMSM sensorless startup control, but also ensures the fast response.

INDEX TERMS Permanent magnet synchronous machine, initial rotor position estimation, symmetric pulse injection, inductance saturation, inverter voltage error.

I. INTRODUCTION

In high performance electrical system driven by Permanent Magnet Synchronous Machines (PMSMs), the precise information of rotor position is required for optimizing voltage and current controls. Without accurate position information during startup process, the motor may suffer from a sudden jitter or short reversal on the shaft. These impacts may deteriorate the acceleration process or more seriously, cause the start failure. The initial rotor position information can be obtained by position sensor measurement results, called sensor-based method, or by sensorless estimation algorithms. The latter one becomes research focus since the normal application has no absolute position sensor and only adopts incremental encoder, or even without encoder. In recent decades, many methods have been proposed to improve the accuracy of the initial position identification in order to ensure smooth and safe startups. Most of them are calculated based on back-EMF, which is called back-EMF based sensorless algorithms.

The machine-saliency-based methods, rather than the back-EMF-based methods, are generally utilized for initial rotor position detection including the standstill. The methods applying continuous-rotating or continuous-pulsating voltage injections have been deeply studied in [1]–[8]. These methods adopt High-Frequency (HF) injections into the machine and modulate the corresponding currents to estimate the rotor position that interact with rotor-position-dependent saliencies. In [1], [2], researchers are partly focusing on the Low Pass Filter (LPF) design during demodulation process, since the filtered signals can be shifted by delays and consequently

The associate editor coordinating the review of this manuscript and approving it for publication was Shihong Ding.

cause position estimation error. In [3] and [4], a zero-sequence carrier voltage between neutral-points and phase windings is utilized to estimate the rotor position. A special phase shift design on injected voltages has been proposed to eliminate the undesirable sixth harmonic by a LPF, so as to compensate estimation error and improve the accuracy. Moreover, some model-based fault diagnosis methods are also widely applied on improving the estimation accuracy of the rotor position [5]–[8]. Most continuous HF injection methods require intensive filtering technology on signal demodulations to get rid of undesirable delays and harmonics, and adopt phase-lock-loop (PLL) controls to converge estimation error to zero. It brings some challenges in filtering design, especially that the filter bandwidth should be suitably designed for varies frequencies and uncertain loads. Therefore, literatures [9]–[12] have made efforts in eliminating the filters and simplify the demodulation procedure. In [9] and [10], direct signal demodulation algorithms such as discrete Fourier transformation and heterodyne technique are adopted to extract estimated position instead of LPF, so that the dynamic performance can be remarkably enhanced with proper system stability design. The continuous square-wave injection methods have demonstrated good dynamic performance since the LPF is eliminated and the signal demodulation process is easy to be realized [11], but it also has the disadvantage that the continuous square wave takes up most of the high-frequency PWM duty cycle and thereby produce current ripple, harmonics, and acoustic noise [12].

To overcome the problem, the impulse voltage injection methods, also known as the Indirect Flux detection by Online Reactance Measurements (INFORM), reduce the injected PWM duty to a smaller value so that the harmonic issue is improved [13]–[15]. The basic idea of the INFORM method is to measure the current response evoked by short voltage space vectors applied in specific directions, and use current variations to directly calculate the rotor position without any filter. This method has the advantage of easy implementation, fast response, low noise and low computation burden [16]. However, there is additional need for instantaneous *di/dt* measurements, so the algorithm requires high speed of current sampling and may be sensitive to the terminal voltage error and inductance error, which are mainly caused by inverter nonlinearity and flux saturation respectively [17]. In [17]–[19], the off-line prediction and on-line complementary injections have been proposed to compensate nonlinear voltage error, but fewer researches have been carried out on the inductance error caused by saturation effect of the magnetizing current [20], [21].

Hence, it is necessary for INFORMs to study the inductance saturation and its compensation principles, which is crucial to the estimation accuracy. In this paper, a modified impulse injection method for identifying initial rotor position is introduced, aiming at eliminating estimation error caused by unbalanced inductance saturation and inverter voltage loss. The resultant current variations under consecutive voltage pulses are associated to the rotor position. Compared with continuous HF injection methods, no filters are needed for extracting the high frequency current signals and the algorithm is insensitive to parameters such as stator resistance and voltage amplitudes. The estimation algorithm is also simple with fast response due to the eliminating of the filter. The proposed method is further developed to reduce the effects of inductance saturation error and inverter nonlinear voltage error on the position estimation accuracy by injecting symmetric voltage pulses iteratively. In Section II, estimation fundamentals for the INFORM are given. The inductance saturation effect and inverter nonlinearity are analyzed in detail and the modified approach is explained in Section III. Various experimental results are given in Section IV. Section V concludes this paper.

II. ANALYSIS OF IMPULSE VOLTAGE INJECTIONS

A. POSITION ESTIMATION BASED ON ROTOR SALIENCY

In PMSM, the principle of initial rotor position estimation is usually associated with rotor salient effect. The saliency is mainly caused by two reasons: one is the non-uniform distribution of magnetic permeability of the rotor lamination which is typically appeared in IPMSM, and the other is the magnetic saturation effect which exists in both SPMSM and IPMSMs. The voltage model considering saliency can be described in stationary $\alpha\beta$ coordinate as

$$\begin{aligned}\begin{bmatrix} u_\alpha \\ u_\beta \end{bmatrix} &= R \cdot \begin{bmatrix} i_\alpha \\ i_\beta \end{bmatrix} \\ &+ \begin{bmatrix} L_{com} + L_{diff}\cos 2\theta_r & L_{diff}\sin 2\theta_r \\ L_{diff}\sin 2\theta_r & L_{com} - L_{diff}\cos 2\theta_r \end{bmatrix} \\ &\cdot p \begin{bmatrix} i_\alpha \\ i_\beta \end{bmatrix} + \omega_r \psi_{PM} \begin{bmatrix} -\cos\theta_r \\ \sin\theta_r \end{bmatrix} \end{aligned} \tag{1}$$

where u, i stands for the stator voltage and stator current in the $\alpha\beta$ reference frame, R is the stator resistance, ω_r is the rotor speed, θ_r is the electrical angle of the rotor, and ψ_{PM} is the peak value of the rotor PM flux linkage. The L_{com} and L_{diff} stand for the common and differential components of dq inductances, which are

$$\begin{cases} L_{com} = \dfrac{L_d + L_q}{2} \\ L_{diff} = \dfrac{L_d - L_q}{2} \end{cases} \tag{2}$$

where L_{d} and L_{q} are the d- and q- axes inductances. It is clear that the value of differential inductance L_{diff} represents the salient degree, and the position information can be extracted from the matrix involving L_{diff}, which is defined as

$$\begin{bmatrix} L_{11} & L_{12} \\ L_{21} & L_{22} \end{bmatrix} = \begin{bmatrix} L_{com} + L_{diff}\cos 2\theta_{\mathrm{r}} & L_{diff}\sin 2\theta_{\mathrm{r}} \\ L_{diff}\sin 2\theta_{\mathrm{r}} & L_{com} - L_{diff}\cos 2\theta_{\mathrm{r}} \end{bmatrix} \tag{3}$$

To detect initial rotor position at standstill, where $\omega_{\mathrm{r}} = 0$, a set of two voltage pulses with same amplitudes are injected

into phase windings [14], and the corresponding voltage equations can be written as

$$\begin{bmatrix} u_{\alpha 1} & u_{\alpha 2} \\ u_{\beta 1} & u_{\beta 2} \end{bmatrix} = R \begin{bmatrix} i_{\alpha 1} & i_{\alpha 2} \\ i_{\beta 1} & i_{\beta 2} \end{bmatrix} + \begin{bmatrix} L_{11} & L_{12} \\ L_{21} & L_{22} \end{bmatrix} p \begin{bmatrix} i_{\alpha 1} & i_{\alpha 2} \\ i_{\beta 1} & i_{\beta 2} \end{bmatrix} \tag{4}$$

where the subscript 1 and 2 stands for the variables under two injections respectively. Therefore, the defined inductance matrix can be calculated as

$$\begin{bmatrix} L_{11} & L_{12} \\ L_{21} & L_{22} \end{bmatrix} = \begin{bmatrix} u_{\alpha 1} - Ri_{\alpha 1} & u_{\alpha 2} - Ri_{\alpha 2} \\ u_{\beta 1} - Ri_{\beta 1} & u_{\beta 2} - Ri_{\beta 2} \end{bmatrix} \times \begin{bmatrix} \frac{\mathrm{d}i_{\alpha 1}}{\mathrm{d}t} & \frac{\mathrm{d}i_{\alpha 2}}{\mathrm{d}t} \\ \frac{\mathrm{d}i_{\beta 1}}{\mathrm{d}t} & \frac{\mathrm{d}i_{\beta 2}}{\mathrm{d}t} \end{bmatrix}^{-1} \tag{5}$$

Note that the inductance matrix contains both sine and cosine value of $2\theta_\mathrm{r}$, as depicted in (3), the estimated rotor electrical angle is

$$\theta_\mathrm{r} = \frac{1}{2}\tan^{-1}\left(\frac{L_{12}+L_{21}}{L_{11}-L_{22}}\right) \pm \frac{\pi}{2} \tag{6}$$

By equation (6) the d-axis direction can be obtained, but the polar information is still implied in symbols $\pm\pi/2$. Thus, the magnet polarity information is further identified by injecting another two reciprocal voltage pulses along the d-axis. Since the two voltage impulses magnetize or demagnetize the flux linkage respectively, the inductances L_d varies differently under two injections. Similarly, the two corresponding currents in the stator are different due to the unbalanced magnetic saturation as well. Therefore, the polarity can be identified by comparing absolute amplitude values of the current. The corresponding current with greater value stands for the direction of north-pole, while the smaller one stands for the south,

$$\theta_e = \begin{cases} \theta_r, & i_{d1} \geq i_{d2} \\ \theta_r + \pi, & i_{d1} < i_{d2} \end{cases} \tag{7}$$

where θ_e is the final estimated rotor electrical angle, $i_{\mathrm{d}1}$ and $i_{\mathrm{d}2}$ are the corresponding currents of the two reciprocal voltage pulses, respectively.

B. CURRENT RESPONSE OF IMPULSE VOLTAGE INJECTIONS

When applying a single PWM voltage on the stator windings at rotor standstill, the response current and its gradient can be derived as

$$i(t) = U(1 - \mathrm{e}^{-(R/L)t})/R \tag{8}$$

$$\frac{\mathrm{d}i(t)}{\mathrm{d}t} = \frac{U}{L}\mathrm{e}^{-(R/L)t} \tag{9}$$

The current sampling mechanism of the controller is normally designed to be discrete. As shown in Fig.1, the controller samples stator current at regular intervals Δt, and

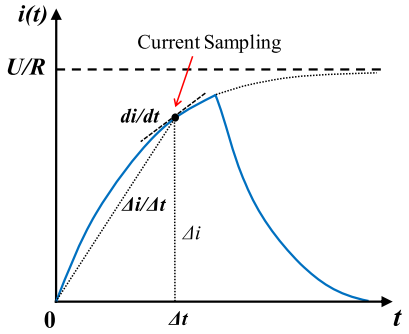

FIGURE 1. Current sampling mechanism of voltage pulse injection.

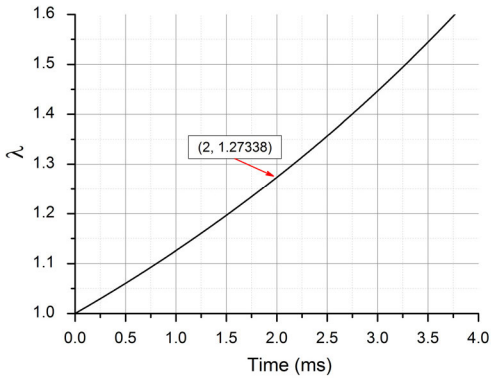

FIGURE 2. Current gradient error with respect to sampling time.

the discrete current variation with respect to time can be expressed as

$$\frac{\Delta i(t)}{\Delta t} = \frac{U}{Rt}[1 - \mathrm{e}^{-(R/L)t}] \tag{10}$$

By comparing (10) with (9), it can be seen that the instantaneous current gradient $\mathrm{d}i/\mathrm{d}t$ is not equal to the average current variation $\Delta i/\Delta t$ during sampling intervals. An error will be introduced by using discrete sampling mechanism, which can be defined as a ratio

$$\lambda(t) = \frac{\Delta i/\Delta t}{\mathrm{d}i/\mathrm{d}t} = \frac{L}{Rt}[\mathrm{e}^{(R/L)t} - 1] \tag{11}$$

By Taylor expansion of (11), the error ratio λ can be expressed as

$$\lambda(t) = 1 + \frac{R}{2L}t + \frac{R^2}{6L^2}t^2 + \varepsilon \tag{12}$$

$$\lim_{t\to 0}\lambda(t) = 1 \tag{13}$$

The error ratio is closely related to the current sampling interval. If the sampling interval is relatively short, the error ratio tends to be 1, and the sampling accuracy will be improved as well. Fig.2 shows the relationship between sampling interval and the error ratio. Taking the 2ms sampling interval as an example, the error ratio is about 1.27.

C. SIMPLIFIED CONCLUSION

In discrete-time controllers, the corresponding currents of the impulse voltage are sampled at interval Δt. By substitute

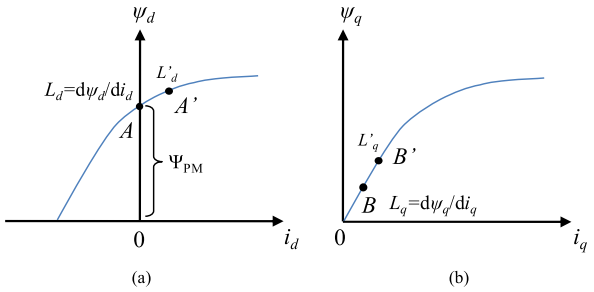

FIGURE 3. Inductance variations due to current injections on dq-axes (a) d-axis magnetization (b) q-axis magnetization.

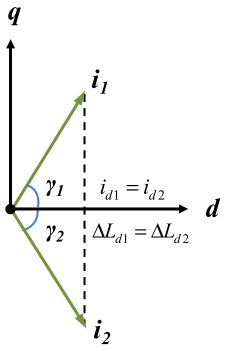

FIGURE 4. Inductance saturation effect due to symmetric magnetization.

average variation current value with gradient current value, the inductance matrix (5) can be rewritten as

$$\begin{bmatrix} L_{11} & L_{12} \\ L_{21} & L_{22} \end{bmatrix} = \frac{\lambda(t)\cdot\Delta t}{(i_{\alpha1}i_{\beta2} - i_{\alpha2}i_{\beta1})} \cdot \begin{bmatrix} u_{\alpha1} - Ri_{\alpha1} & u_{\alpha2} - Ri_{\alpha2} \\ u_{\beta1} - Ri_{\beta1} & u_{\beta2} - Ri_{\beta2} \end{bmatrix} \times \begin{bmatrix} i_{\beta2} & -i_{\alpha2} \\ -i_{\beta1} & i_{\alpha1} \end{bmatrix} \tag{14}$$

Substitute (14) into (6), the estimated position can be simplified as

$$\theta_{\mathrm{r}} = \frac{1}{2}\mathbf{atan2} \quad (Y, X) \pm \frac{\pi}{2} \tag{15}$$

where

$$\begin{cases} Y = u_{\alpha2}i_{\alpha1} + u_{\beta1}i_{\beta2} - u_{\alpha1}i_{\alpha2} - u_{\beta2}i_{\beta1} \\ X = u_{\alpha1}i_{\beta2} + u_{\beta1}i_{\alpha2} - u_{\alpha2}i_{\beta1} - u_{\beta2}i_{\alpha1} \end{cases} \tag{16}$$

The operator should be the four-quadrant inverse tangent Atan2. In (15) and (16), due to the error ratio, the sampling interval and the stator resistance are all reduced, the estimation algorithm is robust and insensitive to system parameters. This performance ensures very flexible requirement of system setting, regardless of the voltage amplitude, the impulse duration or the current sampling time. However, it is important to point out that the two consecutive voltage vectors u_1, u_2 should be linearly independent, to ensure the unique solution of the inductance matrix [15].

III. IMPROVED SYMMETRIC VOLTAGE INJECTION METHOD

A. INDUCTANCES SATURATION ANALYSIS

In PM motor, the stator current applied on d- and q-axes causes different saturation effects on inductances. As shown in magnetization curve of Fig.3, the current i_{d} enhances flux saturation on d-axis from point A to point A' on the magnetization curve, so that the inductance changes from L_{d} to L'_{d}, where $L_{\mathrm{d}} > L'_{\mathrm{d}}$. On the contrary, the q-axis flux is operating on the linear segment BB' of the curve, where the current i_{q} contributes few saturation on the inductance and therefore the value keeps as $L_{\mathrm{q}} = L'_{\mathrm{q}}$.

Considering saturation effect, the inductance variation can be defined as

$$\begin{cases} \Delta L_d = L'_d - L_d = f(i_d) \\ \Delta L_q = L'_q - L_q = 0 \end{cases} \tag{17}$$

$$i_d = i\cos\gamma \tag{18}$$

where the function f represents the non-linear magnetization flux-current curve, i is the amplitude of current vector, and γ is the angle between current vector and the d-axis. Therefore, if the excited currents by double voltage vectors have different saturation effect on d-axis, the estimated position calculated in (6) is needed to be revised according to inductance variations.

To handle this problem, a principle of voltage injection is proposed that the double vectors need to be linearly independent and symmetric about the d-axis [13], and the current vectors are symmetric about the d-axis as well, as shown in Fig.4 where $\gamma_1 = \gamma_2$. As a result, the d-axis current components attribute the same magnetization effect on d-axis flux so that the d-axis inductance variations are equal, which yields

$$\Delta L_d = \Delta L_{d1} = \Delta L_{d2} \tag{19}$$

Then the error of inductance matrix with respect to saturation can be obtained as

$$\begin{cases} \Delta L_{11} = L'_{11} - L_{11} = \dfrac{\Delta L_d}{2}(1 + \cos 2\theta_{\mathrm{r}}) \\ \Delta L_{12} = L'_{12} - L_{12} = \dfrac{\Delta L_d}{2}\sin 2\theta_{\mathrm{r}} \\ \Delta L_{21} = L'_{21} - L_{21} = \dfrac{\Delta L_d}{2}\sin 2\theta_{\mathrm{r}} \\ \Delta L_{22} = L'_{22} - L_{22} = \dfrac{\Delta L_d}{2}(1 - \cos 2\theta_{\mathrm{r}}) \end{cases} \tag{20}$$

Substitute (20) into (6), the revised position can be expressed as

$$\begin{aligned} \theta_r^* &= \frac{1}{2}\tan^{-1}\frac{(L_{12} + \Delta L_{12}) + (L_{21} + \Delta L_{21})}{(L_{11} + \Delta L_{11}) - (L_{22} + \Delta L_{22})} \\ &= \frac{1}{2}\tan^{-1}\frac{L_{12} + L_{12} + \Delta L_d \sin 2\theta_r}{L_{11} - L_{22} + \Delta L_d \cos 2\theta_r} \end{aligned} \tag{21}$$

Comparing (21) with (6), the conclusion can be drawn as

$$\theta_r^* = \theta_r \tag{22}$$

Therefore, the symmetric couple voltage injections achieve no error in estimating the position by using simplified equation (15). It is important to note that the double symmetric voltage vectors should not be both aligned with q-axis since they are linearly correlated. Considering the negative saturation effect and linearly independence, the angle γ is preferred to be ± 45 to ± 60 electrical degrees.

B. DEAD-TIME VOLTAGE LOSS ANALYSIS

In conventional PM motor controls, the voltage applied on stator resistance and inductance are relatively low at rotor standstill. The performance of the estimation algorithm is often influenced by the voltage error caused by inverter dead-time nonlinearities. Due to the existence of the voltage error, the actual amplitude of the injected voltage may be different from the expected value, which can be expressed as

$$u_{AN} = \begin{cases} u_{AN0} - \Delta u_{dead} & (i_a > 0) \\ u_{AN0} + \Delta u_{dead} & (i_a < 0) \end{cases} \tag{23}$$

where the u_{AN} and u_{AN0} are actual and reference phase voltages (e.g. in phase A), and the Δu_{dead} is the dead-time voltage loss. The value of the voltage loss is highly dependent on the dead time, the switching frequency and the dc-bus voltage, and not difficult to calculate and compensate. However, an easier way to eliminate the error is to inject same vectors twice with different amplitudes, where the voltage error does not change during these two similar injections and their differential components satisfy the principle (4) as well:

$$\begin{bmatrix} \Delta u_{\alpha 1} & \Delta u_{\alpha 2} \\ \Delta u_{\beta 1} & \Delta u_{\beta 2} \end{bmatrix} = R \begin{bmatrix} \Delta i_{\alpha 1} & \Delta i_{\alpha 2} \\ \Delta i_{\beta 1} & \Delta i_{\beta 2} \end{bmatrix} + \begin{bmatrix} L_{11} & L_{12} \\ L_{21} & L_{22} \end{bmatrix} \times p \begin{bmatrix} \Delta i_{\alpha 1} & \Delta i_{\alpha 2} \\ \Delta i_{\beta 1} & \Delta i_{\beta 2} \end{bmatrix} \tag{24}$$

where all variables with the prefix Δ represent the differential values of the components. Alternatively, the estimation angle can be rewritten as

$$\theta_{\mathrm{r}} = \frac{1}{2}\mathbf{atan2} \quad (\Delta Y, \Delta X) \pm \frac{\pi}{2} \tag{25}$$

where

$$\begin{cases} \Delta Y = \Delta u_{\alpha 2}\Delta i_{\alpha 1} + \Delta u_{\beta 1}\Delta i_{\beta 2} - \Delta u_{\alpha 1}\Delta i_{\alpha 2} - \Delta u_{\beta 2}\Delta i_{\beta 1} \\ \Delta X = \Delta u_{\alpha 1}\Delta i_{\beta 2} + \Delta u_{\beta 1}\Delta i_{\alpha 2} - \Delta u_{\alpha 2}\Delta i_{\beta 1} - \Delta u_{\beta 2}\Delta i_{\alpha 1} \end{cases} \tag{26}$$

C. IMPLEMENTATION OF THE PROPOSED METHOD

The symmetric voltages injection method is divided into three consecutive steps, as depicted in Fig.5. In the first step, three voltage vectors denoted as u_a, u_b, u_c separating by 120 electrical degrees, are applied along a-, b-, c- phase axes of stator windings with the same amplitudes and the same duration time. The rotor angles can be pre-estimated according to equation (15), utilizing vector combinations of $[(u_a, i_a), (u_b, i_b)]$, $[(u_b, i_b), (u_c, i_c)]$ or $[(u_c, i_c), (u_a, i_a)]$. It is needed to choose one best set of vectors from those three combinations according to the principle, as illustrated

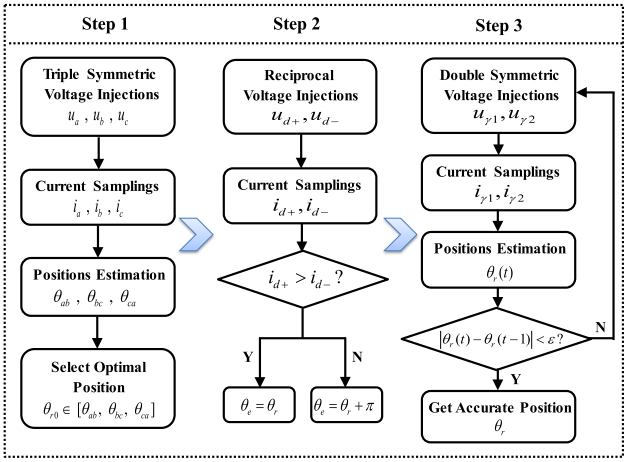

FIGURE 5. Flowchart of proposed method.

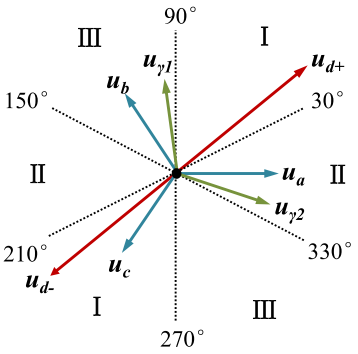

FIGURE 6. Applied voltage vectors with respect to rotor position quadrant.

TABLE 1. Selection principles of voltage vectors.

Rotor position/(°)	Section	Vectors
330~360, 0~30	II	(u_b,i_b), (u_c,i_c)
30~90	I	(u_a,i_a), (u_b,i_b)
90~150	III	(u_c,i_c), (u_a,i_a)
150~210	II	(u_b,i_b), (u_c,i_c)
210~270	I	(u_a,i_a), (u_b,i_b)
270~330	III	(u_c,i_c), (u_a,i_a)

in Fig. 6 and Table 1, that the applied vectors should be symmetric as far as possible about the d-axis which has been pre-classified into six sections. For instance, for the rotor position in section I, combination of vectors $[(u_a, i_a), (u_b, i_b)]$ are preferred. Similarly, vectors $[(u_b, i_b), (u_c, i_c)]$ are chosen in section II and vectors $[(u_c, i_c), (u_a, i_a)]$ are chosen in section III. Then in the second step, two reciprocal voltage pulses u_{d+} and u_{d-} are injected along the directions of θ_{r} and $\theta_{\mathrm{r}} + \pi$, and the polarity can be identified by comparing the absolute values of the current amplitudes, as mentioned in (7) already.

However, since the initial rotor position is random at standstill, the vectors are not perfectly symmetric with the d-axis in most cases, and the estimated position may be inaccurate due

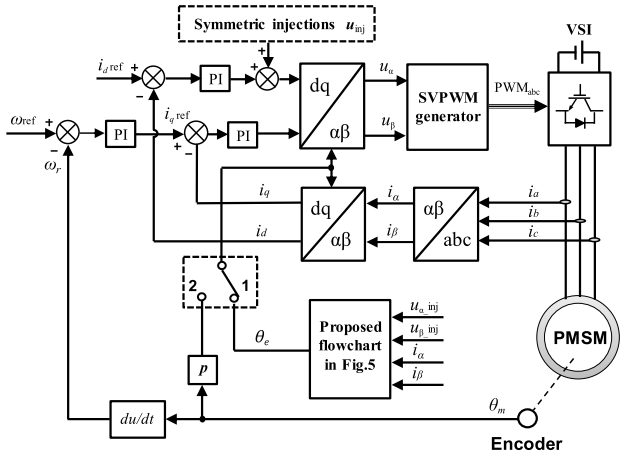

FIGURE 7. Block diagram of the system with symmetric voltage injections for initial rotor identification.

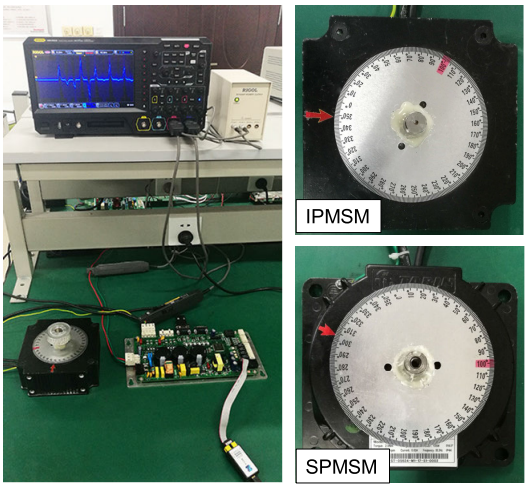

FIGURE 8. Experimental platform, including an IPMSM, a SPMSM and a special designed driver for elevator door applications.

to the unbalanced magnetizations on d-axis. In order to further improve the estimation accuracy, an iterative process of symmetric voltage injections are performed in the third step. According to the last estimated position $\theta_r(t-1)$, a pair of voltages with symmetric offset angles $\pm\gamma$, donated as $u_{\gamma 1}(t)$ and $u_{\gamma 2}(t)$, are injected into the stator windings. The corresponding currents donated as $i_{\gamma 1}(t)$ and $i_{\gamma 2}(t)$ are sampled and the θ_r is updated using (15) as well. By comparison with the two adjacent estimated angles, the convergence condition can be expressed as

$$|\theta_r(n) - \theta_r(n-1)| < \varepsilon \tag{27}$$

where n is the ordinal number of the injections, ε is the preset estimation accuracy threshold. If the result does not meet the convergence condition, another pair of voltages will be applied with the same symmetric angles deviating from the recent estimated position in the anti-clockwise and clockwise direction. Then the comparison between $\theta_r(n+1)$ and $\theta_r(n)$ will be judged again until the absolute error satisfies the convergence condition.

IV. EXPERIMENTAL VERIFICATIONS

The initial position estimation strategy using symmetric voltage injections is tested on an elevator door motor platform. As show in Fig.7, the conventional FOC system embeds the proposed injection algorithm for initial rotor position identification. In Fig.8, the test platform employs an IPMSM, a SPMSM, a STM32F407 series MCU based controller, and a power device designed for elevator door driving system. The IPMSM is used for verifying the proposed method and the SPMSM is used for compatibility comparison. A metal dial is mounted on the shaft for coarse comparison with the real rotor position, and an inner-mounted absolute position sensor AS5408A is used for fine comparison. The parameters of the PMSMs are listed in Table 2.

The amplitude and duration time of the injected voltages should be properly set. With high amplitude and long sampling time, the corresponding currents increase fast and

TABLE 2. PMSM specifications.

IPMSM			
Rated power	43 W	Pole pairs	4
Rated voltage	65 V	Stator resistance	20.6 Ω
Rated current	0.8 A	d-axis inductance	55 mH
Rated torque	2.3 N·m	q-axis inductance	98 mH
Rated speed	180 rpm	Saliency Ratio	1.78
SPMSM			
Rated power	105 W	Pole pairs	10
Rated voltage	220 V	Stator resistance	14.5 Ω
Rated current	0.65 A	d-axis inductance	38 mH
Rated torque	2.0 N·m	q-axis inductance	42 mH
Rated speed	500 rpm	Saliency Ratio	1.11

tend to be unambiguous and robust against noises, so that it can achieve stable estimation results. However, the estimation performance may be deteriorated if the excitations last too long, since the electromagnetic torque driven by large and long lasting currents may cause unexpected rotation, especially under light load conditions. Therefore, by compromising between the estimation accuracy and the drive performance, the voltage injection period has been chosen to be 4ms, which is much less than the rotor response time. After one excitation period, the desired peak value of current has been roughly 0.4A and the corresponding voltage amplitude has found to be 28V. For additional dead-time voltage compensation and pole identification, the voltage amplitude changes to 34V and the current was 0.6A. The switching frequency of the PWM is 15 kHz and the dead-time is set to be 3us.

A. THREE PHASE AXIAL INJECTIONS

In the experiment, the controller outputs three voltage pulses along the A-, B-, C-axes consequently, and the rotor is preset at 12 specific positions with 30 degrees division among one electrical period. Vector combinations of injected voltages and excited currents donated as AB, BC and CA are used to calculate rotor position for three times separately. The results

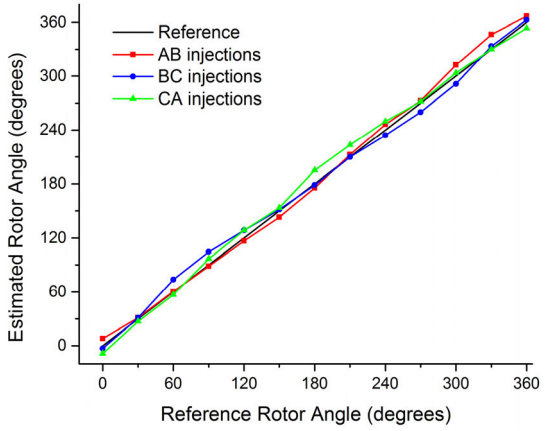

FIGURE 9. Estimated angle based on initial injections.

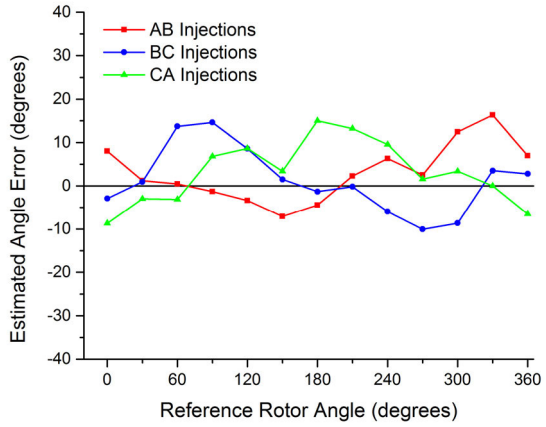

FIGURE 10. Estimated angle error based on initial injections.

show that the estimated error is periodically dependent on the rotor angle, as shown in Fig.9 and Fig.10. The estimation adopting AB-axial injections has better accuracy at position of 60 and 240 degrees, while the estimation using BC- and CA- axial injections have better accuracy at position of 0/180 and 120/300 degrees respectively. These phenomena are consistent with the theoretical derivation in (21) and (22). The identification accuracies at other angles are relatively poor, due to the unbalanced inductance saturation by asymmetric injections. For example, at rotor position of 60 degrees by BC-axial injections, the two consecutive currents cause very unbalanced saturation and the estimated error reaches 15 degrees, while by AB-axial injections the resultant value is almost perfect.

B. ACCURACY IMPROVEMENT BASED ON ITERATION PROCESS

To improve estimation accuracy, voltage pulses are needed to inject symmetrically along the estimated d-axis more than once. The improved method consists of three steps such as the initial injections, the pole-oriented injections and the iterative injections. The first injections along A-, B-, C-axes have the

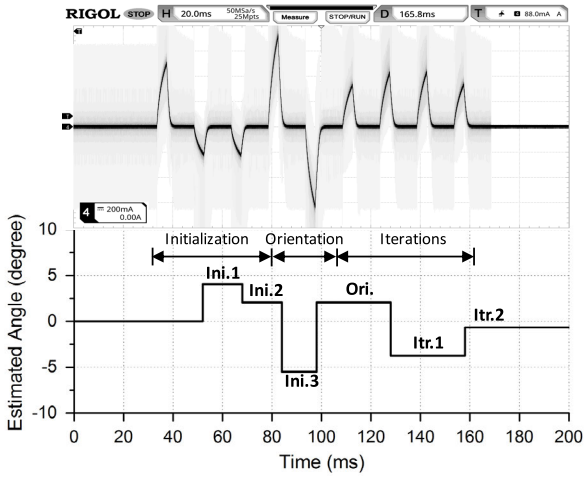

FIGURE 11. Response current and estimated angle at position $\theta_r = 0°$ ($\varepsilon = 0.1$ rad, $u = 28$V).

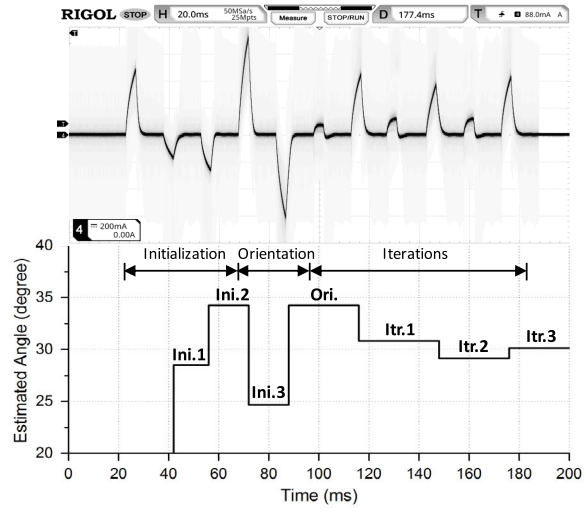

FIGURE 12. Response current and estimated angle at position $\theta_r = 30°$ ($\varepsilon = 0.1$ rad, $u = 28$V).

same amplitudes and durations, and the probable estimated angle can be derived by properly selecting estimated results from the vector combinations. After that, two reciprocal voltages are injected for pole identification. Then groups of vectors are injected symmetrically according to the latest estimated position, and the iterative results converge rapidly.

The completion threshold of the iterative convergence in this test is set to be 0.1 rad (5.73 degrees), which is acceptable in most applications. In Fig.11, the rotor position is preset to be 0 degree at the initial step. Since the BC-axial injections are symmetric about the d-axis, the initial estimation has an accuracy of 2.05 degrees. After pole orientation, the iterative process converges in two periods, and the resultant angle is -0.69 degree. In Fig.12, at preset position of 30 degrees where all axial-directional injections are asymmetric about the angle, the initial estimation obtains relatively poor accuracy at 34.26 degrees. Then the iterative process takes three

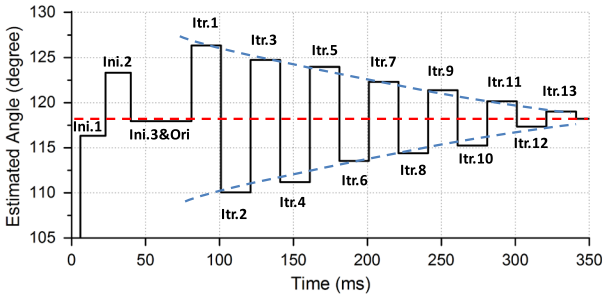

FIGURE 13. Oscillatory iteration process at position $\theta_r = 120°$ ($\varepsilon = 0.01$ rad, $u = 28$V).

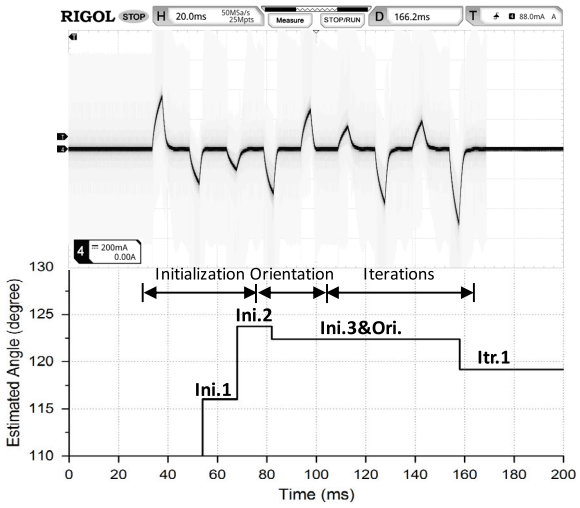

FIGURE 14. Response current and estimated angle with differential injections at position $\theta r = 120°$.

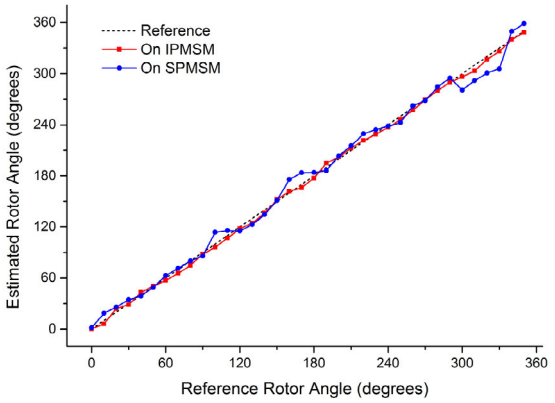

FIGURE 15. Estimated rotor position of proposed method on both IPMSM and SPMSM.

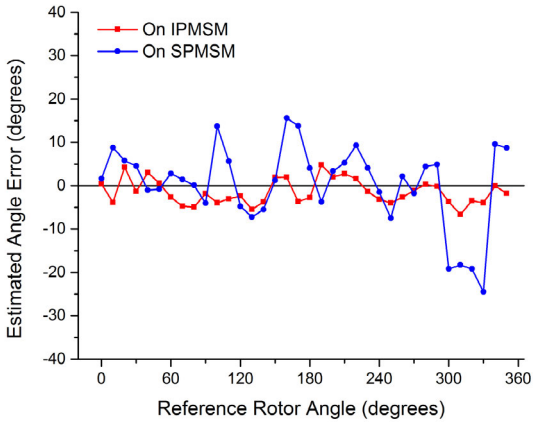

FIGURE 16. Estimated error of proposed method on both IPMSM and SPMSM.

periods and the result converges to an accurate value of 30.14 degrees. In addition, the accuracy could be further improved by reducing the convergence threshold for more iteration periods, as shown in Fig.13. At the specific position of 120 degrees with threshold of 0.01 rad, the resultant angle may have an oscillatory convergence process as the injections developing. However, the convergence condition does not meet after 13 iterations due to the overly strict threshold, and the dead-time voltage error, the current sampling error as well as the unbalanced saturation effect may drive the estimated result away from the truth. A helpful solution is to observe the convergence trajectory and calculate the average value of every two adjacent periods, as shown by the dashed line in Fig.13, when it satisfies

$$\left|\frac{\theta_r(n)+\theta_r(n-1)}{2}-\frac{\theta_r(n-2)+\theta_r(n-3)}{2}\right|<\varepsilon \quad (28)$$

the final estimated angle can be obtained by

$$\theta_{r\_final}=\frac{1}{2}[\theta_r(n)+\theta_r(n-1)] \quad (29)$$

To further improve estimation accuracy, dead-time voltage loss should be compensated. In Fig.14, the injections in iteration process are repeated twice with voltage amplitudes of 28V and 34V respectively, and the difference components are used to calculate the angle. Comparing with the iteration process in Fig.13, the iteration process in Fig.14 finishes rapidly in just one period, and the rotor position estimation accuracy is enhanced with good tracking as well.

C. VERIFICATION AND LIMITATION OF PROPOSED METHOD ON FULL POSITION RANGE

The proposed method is verified by traversing the preset angle along 360 degrees on both IPMSM and SPMSM. All experimental setups are the same except the test motors with different saliencies. As can be observed from Fig.15, the resultant angle curves are consistence with the reference values on both two types of motors. In Fig.16, the maximum deviation of the angle error in IPMSM (rectangular dot line) is 5.5 degrees and the standard deviation is 2.83 degrees. By comparison, the round dot line shows maximum deviation of 25 degrees on SPMSM, whose deviation is larger than that in IPMSM. Furthermore, some obvious distortions occur near 300 degrees on the curve, which reveal the disadvantage of precision limit when applied in low saliency PMSMs. Normally, these special distortion errors are caused by sampling noise when one of the current values expressed in $\alpha\beta$ stationary frame is close to zero, and the estimated

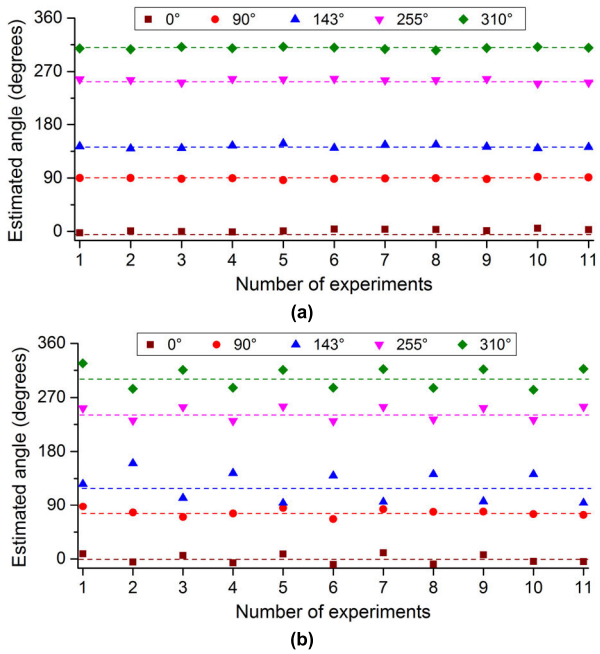

FIGURE 17. Stability and consistency of proposed method at specific positions (a) IPMSM (b) SPMSM.

error is amplified by the obscure inductance differences. In Fig.17 (a), the injection process is repeated several times at some specific positions on the IPMSM whose saliency ratio is 1.78, and good consistency and repeatability are proved by all the estimated results. Contrarily, as shown in Fig.17 (b), the estimation results on SPMSM with saliency ratio 1.11 are not converged. However, the distributions of the dots are symmetric with the real positions (dash lines), which is similar to the oscillatory phenomenon in Fig.13, so precise results can be achieved by (28) and (29) as well. Therefore, it can be concluded that the difference between L_d and L_q is the key factor on the estimation accuracy and stability. The low dq inductance difference in SPMSM makes the response currents very similar, so that the current noise and voltage error are more significant. However, by utilizing inductance saturation effect, the proposed current injection method is proved to be available for both IPMSM and SPMSM.

V. CONCLUSION

This paper proposed an improved estimation method of initial rotor position based on symmetric pulsating injections for IPMSM drives. A series of phase-axial voltage pulses are injected into phase windings to calculate the probable rotor position and its orientation at first. Then additional iterative process of symmetric voltage injections was put forward to approximate the real position rapidly. To the proposed estimated method, the conclusions can be drawn:

1) The precision of rotor position can reach 1.6% by rough detection within 80ms, and can be further improved to 0.1% by fine detection.

2) The position deviation is minimized since the negative effects caused by unbalanced inductance saturation and dead-time voltage loss can be efficiently reduced.

3) It can have accurate and stable performance to IPMSM with the saliency ratio of 1.78, but has some defects in SPMSM due to its low saliency ratio of 1.11.

4) More future work should be carried out on the mechanism of estimation error with respect to the rotor saliency and sampling errors. Further algorithmic processing is also needed to improve the compatibility of the method on SPMSM.

REFERENCES

[1] J. M. Liu and Z. Q. Zhu, "Novel sensorless control strategy with injection of high-frequency pulsating carrier signal into stationary reference frame," *IEEE Trans. Ind. Appl.*, vol. 50, no. 4, pp. 2574–2583, Jul. 2014.
[2] Q. Tang, A. Shen, X. Luo, and J. Xu, "PMSM sensorless control by injecting HF pulsating carrier signal into ABC frame," *IEEE Trans. Power Electron.*, vol. 32, no. 5, pp. 3767–3776, May 2017.
[3] A. H. Almarhoon, Z. Q. Zhu, and P. Xu, "Improved rotor position estimation accuracy by rotating carrier signal injection utilizing zero-sequence carrier voltage for dual three-phase PMSM," *IEEE Trans. Ind. Electron.*, vol. 64, no. 6, pp. 4454–4462, Jun. 2017.
[4] P. Xu and Z. Q. Zhu, "Initial rotor position estimation using zero-sequence carrier voltage for permanent-magnet synchronous machines," *IEEE Trans. Ind. Electron.*, vol. 64, no. 1, pp. 149–158, Jan. 2017.
[5] K. Mei and S. Ding, "Second-order sliding mode controller design subject to an upper-triangular structure," *IEEE Trans. Syst., Man, Cybern., Syst.*, early access, Nov. 5, 2018, doi: 10.1109/TSMC.2018.2875267.
[6] Y. Wu, B. Jiang, and N. Lu, "A descriptor system approach for estimation of incipient faults with application to high-speed railway traction devices," *IEEE Trans. Syst., Man, Cybern., Syst.*, vol. 49, no. 10, pp. 2108–2118, Oct. 2019.
[7] K. Shi, W. Song, H. Ge, P. Xu, Y. Yang, and F. Blaabjerg, "Transient analysis of microgrids with parallel synchronous generators and virtual synchronous generators," *IEEE Trans. Energy Convers.*, vol. 35, no. 1, pp. 95–105, Mar. 2020.
[8] K. Shi, H. Ye, P. Xu, D. Zhao, and L. Jiao, "Low-voltage ride through control strategy of virtual synchronous generator based on the analysis of excitation state," *IET Gener., Transmiss. Distrib.*, vol. 12, no. 9, pp. 2165–2172, May 2018.
[9] X. Zhang, H. Li, S. Yang, and M. Ma, "Improved initial rotor position estimation for PMSM drives based on HF pulsating voltage signal injection," *IEEE Trans. Ind. Electron.*, vol. 65, no. 6, pp. 4702–4713, Jun. 2018.
[10] S.-I. Kim, J.-H. Im, E.-Y. Song, and R.-Y. Kim, "A new rotor position estimation method of IPMSM using all-pass filter on high-frequency rotating voltage signal injection," *IEEE Trans. Ind. Electron.*, vol. 63, no. 10, pp. 6499–6509, Oct. 2016.
[11] Y.-D. Yoon, S.-K. Sul, S. Morimoto, and K. Ide, "High-bandwidth sensorless algorithm for AC machines based on square-wave-type voltage injection," *IEEE Trans. Ind. Appl.*, vol. 47, no. 3, pp. 1361–1370, May/Jun. 2011.
[12] X. Wu, Y. Feng, X. Liu, S. Huang, X. Yuan, J. Gao, and J. Zheng, "Initial rotor position detection for sensorless interior PMSM with square-wave voltage injection," *IEEE Trans. Magn.*, vol. 53, no. 11, Nov. 2017, Art. no. 8112104.
[13] E. Robeischl and M. Schroedl, "Optimized INFORM measurement sequence for sensorless PM synchronous motor drives with respect to minimum current distortion," *IEEE Trans. Ind. Appl.*, vol. 40, no. 2, pp. 591–598, Mar./Apr. 2004.
[14] C. Wang and L. Xu, "A novel approach for sensorless control of PM machines down to zero speed without signal injection or special PWM technique," *IEEE Trans. Power Electron.*, vol. 19, no. 6, pp. 1601–1607, Nov. 2004.
[15] M. Schroedl, "Sensorless control of AC machines at low speed and standstill based on the 'INFORM' method," in *Proc. 31st IEEE IAS Annu. Meeting, Conf. Rec.*, vol. 1, Oct. 1996, pp. 270–277.

[16] R. Ni, K. Lu, F. Blaabjerg, and D. Xu, "A comparative study on pulse sinusoidal high frequency voltage injection and INFORM methods for PMSM position sensorless control," in *Proc. 42nd Annu. Conf. IEEE Ind. Electron. Soc. (IECON)*, Oct. 2016, pp. 2600–2605.
[17] G. Xie, K. Lu, and S. K. Dwivedi, "Minimum-voltage vector injection method for sensorless control of PMSM for low-speed operations," *IEEE Trans. Power Electron.*, vol. 31, no. 2, pp. 1785–1794, Feb. 2016.
[18] J. M. Guerrero, M. Leetmaa, F. Briz, A. Zamarron, and R. D. Lorenz, "Inverter nonlinearity effects in high-frequency signal-injection-based sensorless control methods," *IEEE Trans. Ind. Appl.*, vol. 41, no. 2, pp. 618–626, Mar/Apr. 2005.
[19] G. Xie, K. Lu, S. K. Dwivedi, and J. R. Rosholm, "Improved INFORM method by minimizing the inverter nonlinear voltage error effects," in *Proc. IEEE Workshop Electr. Mach. Design, Control Diagnosis (WEMDCD)*, Mar. 2015, pp. 188–194.
[20] K. Lu, X. Lei, and F. Blaabjerg, "Artificial inductance concept to compensate nonlinear inductance effects in the back EMF-based sensorless control method for PMSM," *IEEE Trans. Energy Convers.*, vol. 28, no. 3, pp. 593–600, Sep. 2013.
[21] H. Zhaobin, Y. Linru, and W. Zhaodong, "Sensorless initial rotor position identification for non-salient permanent magnet synchronous motors based on dynamic reluctance difference," *IET Power Electron.*, vol. 7, no. 9, pp. 2336–2346, Sep. 2014.

ZIHUI WANG received the B.S. and Ph.D. degrees in electrical engineering from Zhejiang University, Hangzhou, China, in 2007 and 2012, respectively.

From 2009 to 2011, he was a Research Assistant with the University of Aalborg, Aalborg, Denmark. In 2012, he was with the Research Center of Philips Co., Ltd., Shanghai, China, as a Researcher. In 2013, he became a Lecturer with the Department of Automation and Engineering, Zhejiang University of Science and Technology, Hangzhou, China. From 2016 to 2019, he was a Postdoctoral Researcher with Zhejiang University, Hangzhou, China. His research interests include control of power electronic systems and control of permanent magnet synchronous machines with sensorless algorithms.

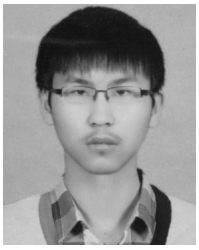

ZEWEI CAO received the B.S. degree in automation from the Zhejiang University of Science and Technology, Hangzhou, China, in 2018, where he is currently pursuing the M.S. degree in automobile engineering.

His research interests include vehicle electrical appliances and automatic control and electric drive control technology.

ZHIYUAN HE received the B.S. and M.S. degrees in electrical engineering from Zhejiang University, Hangzhou, China, in 1983 and 2000, respectively.

From 1996 to 1997, he was a Research Assistant with the Technical University of Munich, Germany. From 2003 to 2004, he was a Visiting Scholar with the Institute of power electronics, Technical University of Berlin, Germany. Since 2007, he has been a Professor with the School of Automation and Electrical Engineering, Zhejiang University of Science and Technology, Hangzhou, China. His research interests include electrical engineering and power electronics. Since 2009, he has been the Vice President of the Zhejiang Provincial Power Supply Society, China.